Switching Characteristics of a 4H-SiC IGBT with Interface Defects Up to the Nonquasi-Static Regime

Iliya Pesic[1,2], Dondee Navarro[2], Masato Fujinaga[2], Yoshiharu Furui[2], and Mitiko Miura-Mattausch[1]

[1] Hiroshima University, 1-3-1 Kagamiyama, Higashi-Hiroshima 739-8530 Japan
Phone: +81-824-24-7637 E-mail: iliya.pesic@gmail.com
[2] Silvaco Japan, 4F Miyake Bldg, 549-2 Shinano-cho, Totsuka, Yokohama 244-0801 Japan

Abstract

The switching characteristics of a 4H-SiC IGBT with interface defects are analyzed up to the non-quasi-static (NQS) regime using reported interface density measurements and device simulation. A threshold voltage shift and current degradation are observed under quasi-static (QS) condition. At fast switching, the trapping effect is observed as a surge of current at the initial gate voltage switch-on, and the NQS behavior itself conceals the trapping effect.

1. Introduction

The 4H-SiC/SiO$_2$ interface has a high interface defect density D_{it} characterized by distinct deep and shallow traps as shown in the measurements in Fig. 1 [1]. The previous work of the author investigated the effects of the measured interface density on the static threshold characteristics of a 4H-SiC IGBT device shown in Fig. 2. The collector current I_c is severely degraded. The deep trap D_{1a} causes the threshold voltage to shift to higher gate voltages while the shallow trap D_{2a} causes current degradation as shown in Fig 3a and b [2].

The extension from static to transient analysis, however, is not straightforward. The static results cannot be used directly to predict transient device characteristics because the dynamics of carriers are governed not only by the applied voltages but also by: (1) the time to charge/discharge the channel and base regions, and (2) the time for trapping/detrapping of carriers due to interface defects. It is the aim of this work to characterize the dynamic response of 4H-SiC IGBT in the presence of traps when fast switching is applied with the device simulation. The work is relevant since power devices are mainly used as switches in power circuits.

2. Transient Device Simulation with Measured Defects

Device simulation involves solving the Poisson equation consistently with the continuity equations to describe the carrier dynamics [3]. The space charge density ρ which is the sum of all contributing charges is

$$\rho = q\left(p - n + N_D^+ + N_A^-\right) + Q_T \tag{1}$$

where q is the unit electronic charge, p is the concentration of holes, n is the concentration of electrons, N_D is the concentration of ionized donors, N_A is the concentration of ionized acceptors, and Q_T is the density of charges due to contributions from interfacial trap states. The defects existing within the bandgap as reported in the measurement are included as interface defects. For this work, only the acceptor-like traps D_{1a} and D_{2a} are considered because the carriers in the device are electrons. D_{1a} is modeled as a

Gaussian distribution as

$$g_{GA}(E) = NGA \cdot \exp\left[-\left(\frac{EGA - E}{WGA}\right)^2\right] \tag{2}$$

where E is the energy level of the trap state, EGA is the energy level where the distribution peaks, NGA is the trap density per unit energy at the peak of the distribution and WGA is the characteristic decay energy for the distribution.

D_{2a} near the conduction band edge is modeled as an exponential distribution given by

$$g_{TA}(E) = NTA \cdot \exp\left(\frac{E - E_c}{WTA}\right), \tag{3}$$

where E_c is the energy at the semiconductor conduction band edge, NTA is the trap density per unit energy at the semiconductor conduction band edge and WTA is the characteristic decay energy. The values of the constants in the equations are extracted from the reported measurement.

The total contribution from the defect states to the charge density is then calculated as $p_T = p_{TA} + p_{GA}$

$$p_{TA} = \int_{E_V}^{E_C}\left\{g_{TA}(E) \cdot f_{t,TA}(E, n, p)\right\} dE \tag{4}$$

$$p_{GA} = \int_{E_V}^{E_C}\left\{g_{GA}(E) \cdot f_{t,GA}(E, n, p)\right\} dE \tag{5}$$

where $f_{t,TA}$ and $f_{t,GA}$ are the probabilities of occupation of a trap level at energy E for the exponential and Gaussian acceptor and donor states. $f_{t,TA}$ is given as

$$f_{t,TA} = \frac{v_n \cdot SIGTAE \cdot n + v_p \cdot SIGTAH \cdot n_i \exp\left[\frac{E_i - E}{kT}\right]}{v_n \cdot SIGTAE \cdot \left(n + n_i \exp\left[\frac{E - E_i}{kT}\right]\right) + v_p \cdot SIGTAH \cdot \left(p + n_i \exp\left[\frac{E_i - E}{kT}\right]\right)} \tag{6}$$

In the transient simulation case, additional rate equation is given for p_{TA} and p_{GA}. For p_{TA},

$$\frac{d}{dt}(p_{TA}) = \int_{E_v}^{E_C} g_{TA}(E)\left[v_n \cdot SIGTAE\left(n(1 - f_{t,TA}(E)) - f_{t,TA}(E)n_i \exp\left[\frac{E - E_i}{kT}\right]\right)\right.$$
$$\left. - v_p \cdot SIGTAH\left(p \cdot f_{t,TA}(E) - (1 - f_{t,TA}(E))n_i \exp\left[\frac{E_i - E}{kT}\right]\right)\right] dE \tag{7}$$

Similar forms of Eq. 6 and 7 are followed for $f_{t,GA}$ and p_{GA}, respectively.

A step function of varying rise times and gate voltages is used as input. The collector voltage V_c is fixed to 15V to ensure current conduction for switching evaluation. The capture cross section parameters are set to 1e18.

3. Results and Discussion

Fig. 4a shows the transient current at V_g=25V with a slow input rise time t_{rise} of 20μs. For slow switching, the current with combined D_{1a} and D_{2a} starts to increase according to the applied V_g with the waveform showing no trapping effects. A surge of current becomes visible due to carriers being trapped until it decays and reaches the static

value in Fig. 3b. The shallow trap D_{2a} introduced a larger influence to degrade the current because the high density of carriers is in the conduction band where D_{2a} is located.

At t_{rise} = 200ns, the surge of current is bounded by the transient current without the defects as shown in Fig. 4b. This current without defects is governed only by the dynamics of charging/discharging of the channel and base, or the nonquasi-static (NQS) characteristics. This means that the magnitude of current due to the trapping effect is limited by the NQS current.

Fig. 5a shows the current characteristics with total defects for different switching times at the NQS regime. The initial surges are all bounded by the NQS current. Fig. 5b shows the switching characteristics as a function of normalized transient time by t_{rise}. Due to the stronger NQS effect the current decay occurs much later for faster switching. The NQS effect observed for the t_{rise} =1000ns occurs frequently for normal device operation conditions. The observed phenomena are summarized in Fig. 6. The maximum effect of trapping is governed by the NQS current. Therefore, any measurement of current with carrier trapping in the static case (quasi-static or QS approximation) does not necessarily appear as degradation in the transient current during switching. Calculation of transient current using QS with trapping effects introduces a maximum difference of $\Delta I = I_{QS} - I_{NQS}$. In compact modeling, $I_{NQS} = I_{QS} + \mathrm{d}Q/\mathrm{d}t$ where Q is the charge responsible for charging. So a first-order approximation of ΔI gives $\mathrm{d}Q/\mathrm{d}t$, which is the charging current. This correction is important in circuit simulation for correct prediction of waveform of SiC-IGBT during switching characteristics.

4. Summary

Investigation of the switching characteristics of a 4H-SiC IGBT with interface defects showed threshold voltage shift and current degradation under quasi-static (QS) condition. At nonquasi-static (NQS) switching, the surge of current due to trapping effects is concealed by the NQS current. The NQS behavior itself limits the trapping of carriers.

References

[1] V. V. Afanasev, et al, *Phys. Stat. Sol. (a)* 162, 321 (1997).
[2] I. Pesic, et al, *Int'l Semiconductor Device Res. Symp.* (2013).
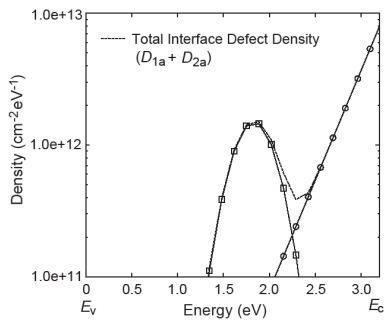[3] *ATLAS User's Manual*, SILVACO, Inc. (2014).

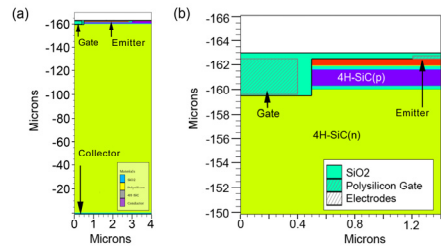Fig. 1. SiC/SiO$_2$ measured interface defect density [1].

Fig. 2. SiC-IGBT device structure (a) Cross-section (b) Channel region of the SiC-IGBT device structure used in the simulation.
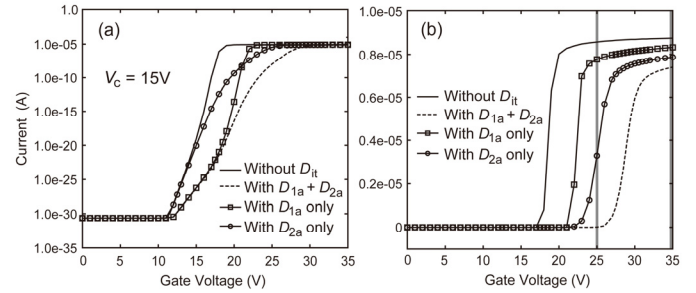

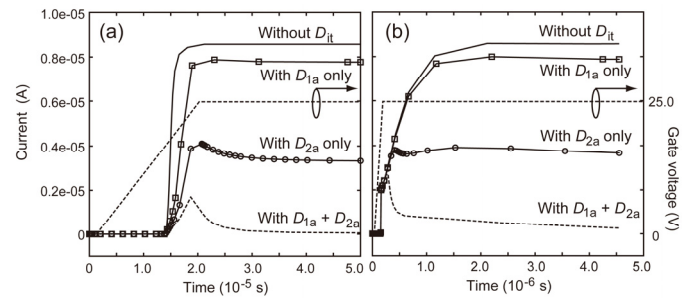Fig. 3a and b. Effect of defects on static current. Log and linear plots.

Fig. 4. Transient current characteristics at V_g = 25V. (a) Slow input rise time = 20μs and (b) fast input rise time = 200ns.
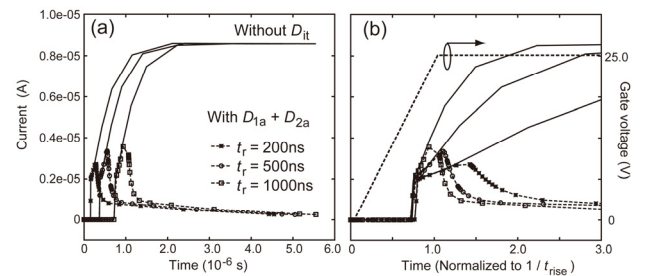

Fig. 5. Transient current characteristics at V_g = 25V and varying input rise times.
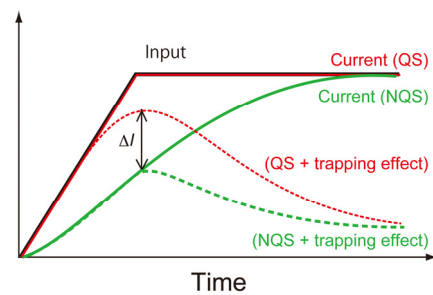

Fig. 6. Schematic illustration of transient current with the interplay of NQS and carrier trapping effects.